

## Supplementary Information for

### Two-dimensional co-crystallization of two carboxylic acid derivatives having dissimilar symmetries at the liquid/solid interface

Qiu Liang,<sup>a</sup> Yanxia Yu,<sup>bc</sup> Guangyuan Feng,<sup>a</sup> Yongtao Shen,<sup>a</sup> Ling Yang<sup>d</sup> and Shengbin Lei<sup>\*a</sup>

<sup>a</sup>Tianjin Key Laboratory of Molecular Optoelectronic Science, Department of Chemistry, School of Science & Collaborative Innovation Center of Chemical Science and Engineering (Tianjin), Tianjin University, Tianjin 300072, P. R. China

<sup>b</sup>Jiangxi University of Science and Technology, Ganzhou 341000, P. R. China

<sup>c</sup>MOE of the Key Laboratory of Bioinorganic and Synthetic Chemistry The Key Lab of Low-carbon Chem and Energy Conservation of Guangdong Province, School of Chemistry, Sun Yat-Sen University Guangzhou 510275, P. R. China

<sup>d</sup>School of Chemistry and Chemical Engineering, Harbin Institute of Technology, Harbin 150080, People's Republic of China

\*Email: shengbin.lei@tju.edu.cn

## 1. Experimental Section

Commercially available n-octanoic acid, 4,4',4'',4'''-(1,4-phenylenebis(pyridine-6,2,4-triyl))tetrabenzoic acid (PBPTTBA) and 1,3,5-tris(4-carboxyphenyl)benzene (BTB) were purchased from Jilin Chinese Academy of Sciences-Yanshen Technology Co., Ltd. and used without further treatment. Highly oriented pyrolytic graphite (HOPG) substrates were freshly cleaved using adhesive tape. Stock solutions of PBPTTBA (saturated,  $< 1 \times 10^{-4}$  M) and BTB ( $4.16 \times 10^{-5}$  M) were prepared by separately dissolving an appropriate amount of solid sample in n-octanoic acid. Then the as-prepared PBPTTBA and BTB solutions were mixed together with specific ratios, followed by drop-casting 5  $\mu$ L of the mixing solution on a freshly cleaved HOPG surface. After the treatments, the samples were studied by scanning tunneling microscope (STM) with its tip immersed directly into the droplet. The STM observations were carried out at the liquid/solid interface for all cases by using Bruker scanning probe microscopy under ambient conditions, and the tips were mechanically cut Pt/Ir (80/20) wires. All the STM images were recorded using constant current mode, and the specific tunneling conditions were illustrated in the corresponding figure captions. The calibration of the STM images was performed by using the HOPG lattice with atomic resolution.

## 2. Computational details

To get insight into driving force of the co-assembly of 4,4',4'',4'''-(1,4-phenylenebis(pyridine-6,2,4-triyl)) tetrabenzoic acid (PBPTTBA) and 1,3,5-tris(4-carboxyphenyl) benzene (BTB), simulation were performed by using density functional theory B3LYP method combined with the 3-21G basis sets for all the atoms [1-3]. Two polygonal networks, compressed hexagon in crystal A and quasi-hexagon in crystal B were focused on. To keep the hexagon skeleton in plain as on the surface, the carbon atom of the benzene ring, connected to the COOH group, is fixed

during the optimization processes. All calculations were carried out using the Gaussian 03 programs [4] and the optimized geometries for the ideal and deviated hydrogen bonds in cocrystal A and B are drawn by using the GaussView [5] shown in Fig S7. The compressed hexagon composed by two PBPTTBA molecules and two BTB molecules with ideal R<sup>2</sup>2(8) 180° hydrogen bonding (Fig S7a) is a little more stable than the quasi-hexagon composed of three PBPTTBA molecules and two BTB molecules with one edge formed by the 1,4-bis(4-pyridyl)benzene backbone of PBPTTBA (Fig S7b) and with hydrogen bond deviated from the 180°. The binding energy of each hydrogen bonding pair ( $E_{\text{HBP}}$ ) of the former is -1.465 eV, 0.018 eV lower than that of the later. It implies that the deviation leads unnoticing contribution to the stability of the hydrogen bond and the polygonal networks.

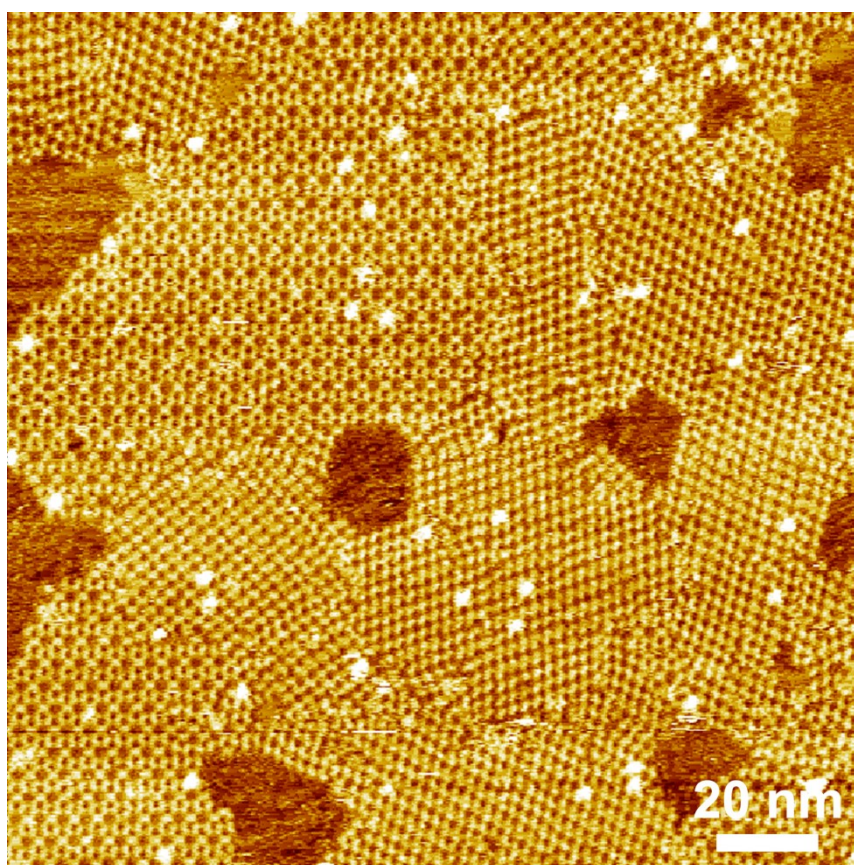


Figure S1. Large-scale self-assembling structure of PBPTTBA (scan size: 168×168 nm<sup>2</sup>). Imaging conditions:  $V_{\text{bias}} = -600$  mV,  $I_{\text{set}} = 330$  pA.

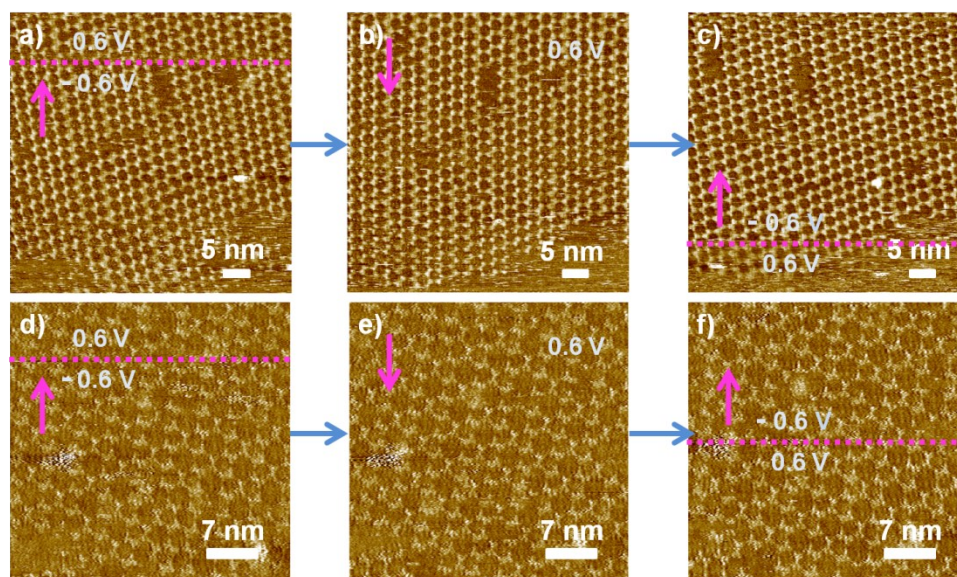


Figure S2. Sequential STM images showing no structure transition for PBPTTBA by reversing the polarity of the substrate bias. (a)-(c) Quadrilateral tiling of PBPTTBA. (b)-(f) Kagomé structure of PBPTTBA. Imaging conditions:  $V_{\text{bias}} = -600 \text{ mV}$ ,  $I_{\text{set}} = 330 \text{ pA}$ .

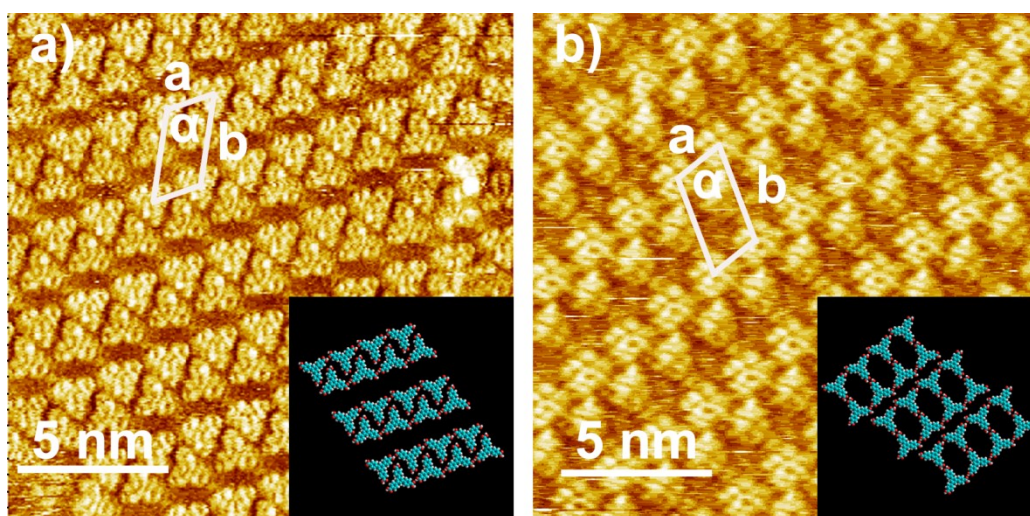


Figure S3. The close-packed structures of BTB at the octanoic acid/HOPG interface ( $C_{\text{BTB}} = 4.16 \times 10^{-4} \text{ M}$ ). Imaging conditions:  $V_{\text{bias}} = -600 \text{ mV}$ ,  $I_{\text{set}} = 330 \text{ pA}$ .

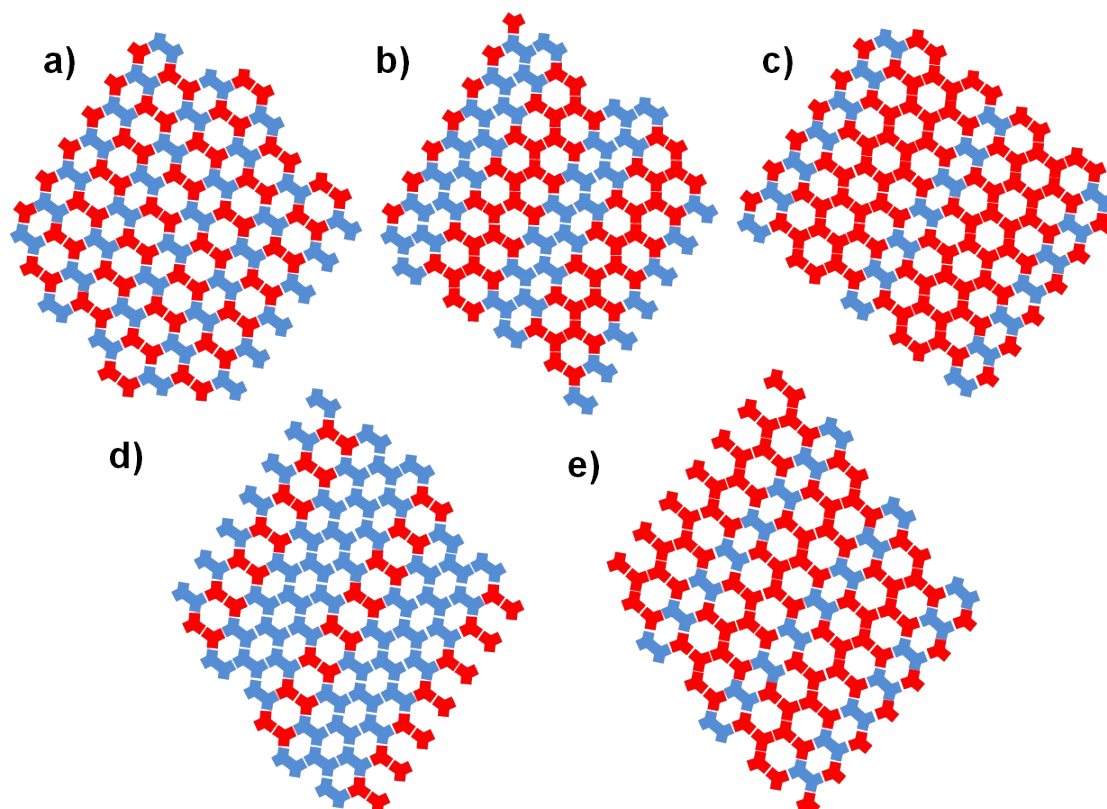


Figure S4. Some possible binary networks where PBPTTBA(blue) and BTB(red) connected to each other via ideal homomeric or heteromeric  $R^2_2(8)$  hydrogen bonding.

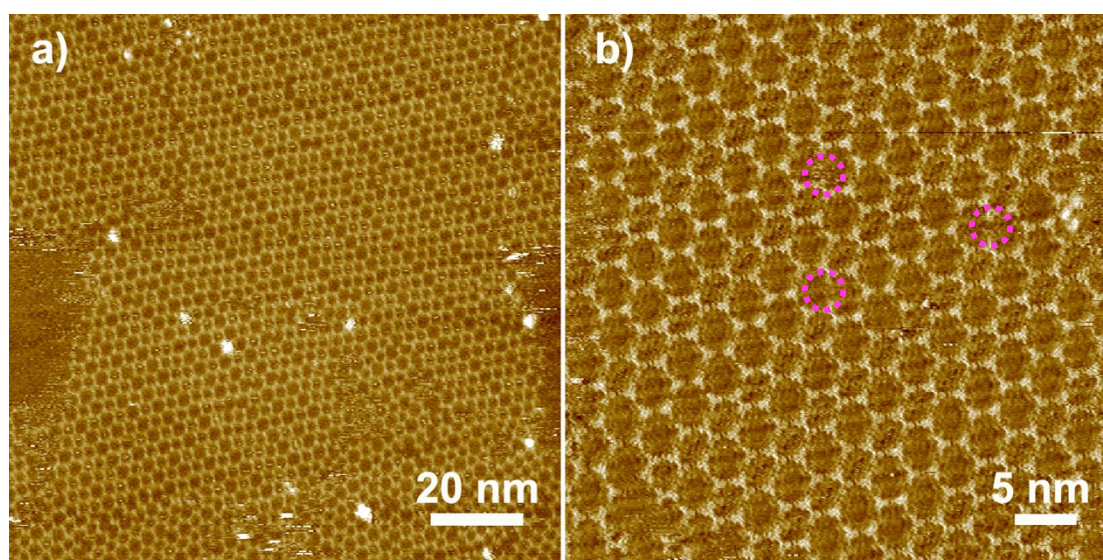


Figure S5. Large-scale co-assembled structures in which hydrogen bond is formed under an energetically ideal bonding angle of  $180^\circ$  between PBPTTBA and BTB (scan size: a)  $120 \times 120 \text{ nm}^2$ ; b)  $46 \times 46 \text{ nm}^2$ ). Imaging conditions:  $V_{\text{bias}} = -600 \text{ mV}$ ,  $I_{\text{set}} = 330 \text{ pA}$ . Some absence of molecules is marked by purple dotted circle.

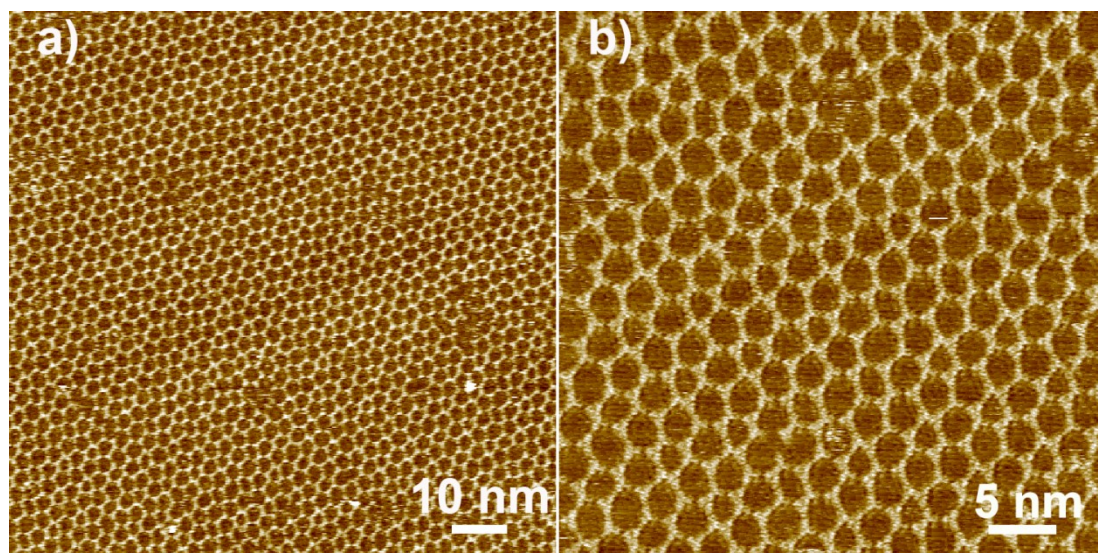


Figure S6. Large-scale STM image of cocrystal B (scan size: a)  $100 \times 100 \text{ nm}^2$ ; b)  $42 \times 42 \text{ nm}^2$ ). Imaging conditions:  $V_{\text{bias}} = -600 \text{ mV}$ ,  $I_{\text{set}} = 330 \text{ pA}$ .

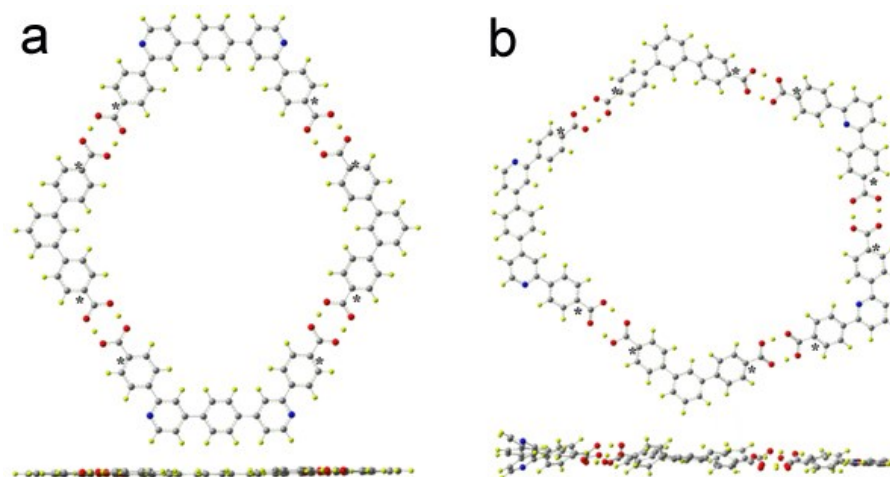


Figure S7. Optimized configuration of the ideal and deviated hydrogen bonds in cocrystal A (a) and B (b), the average energies of each hydrogen bond pair ( $E_{\text{HBP}}$ ) are  $-1.465$  and  $-1.447 \text{ eV}$ , which indicates the deviation from  $180^\circ$  only brings minor effect to the stability of the  $R^2_2(8)$  hydrogen bonds.

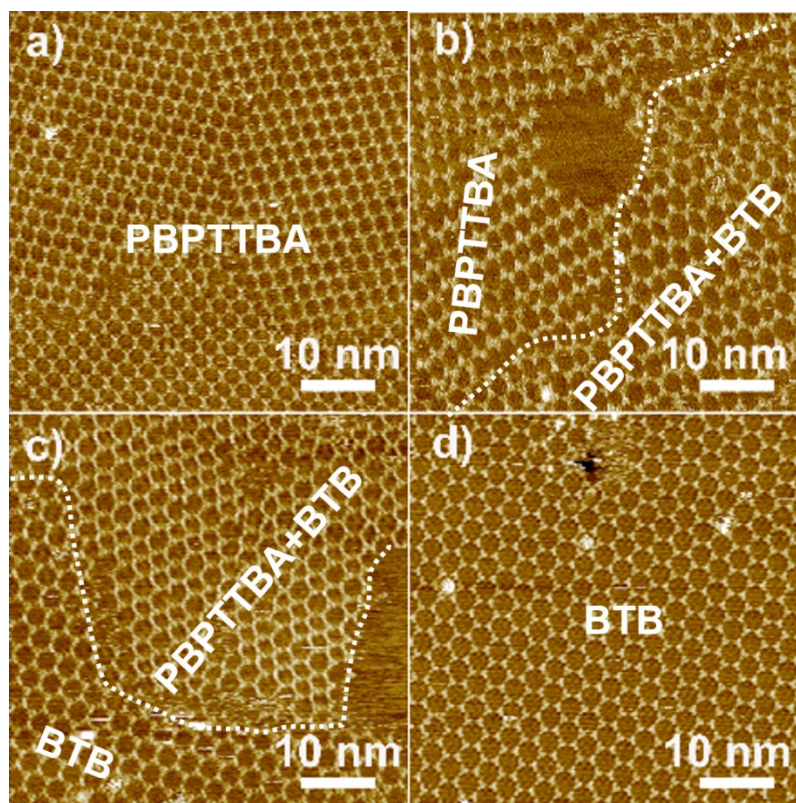


Figure S8. Typical STM images of the adlayer formed by PBPTTBA and BTB. The ratio of PBPTTBA to BTB in the solution is a) 2:1, b) 3:2, c) 2:3, and d) 1:2. Imaging conditions:  $V_{\text{bias}} = -600$  mV,  $I_{\text{set}} = 330$  pA.

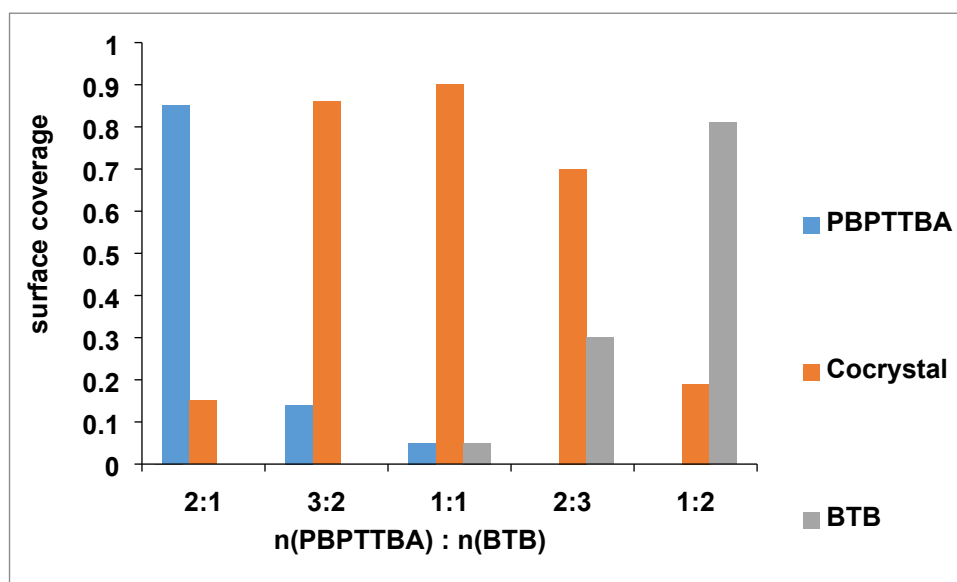


Figure S9. Observed different structural proportions at different molar ratio (PBPTTBA:BTB).

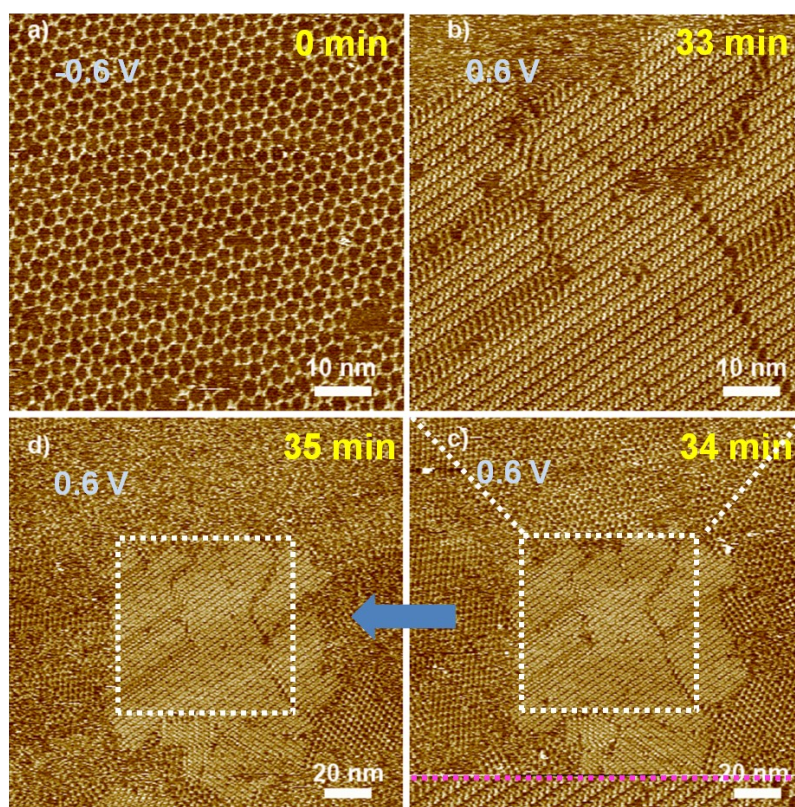


Figure S10. a-b) Sequential STM images showing the phase transition from cocrystal B to the preferentially adsorbed BTB. c) Large-scale STM image immediately captured after recording the small area STM image provided in panel b). d) Continued STM scan in the sequence of panel c). In Figure c, scanning direction is from bottom to top, and the purple dotted line indicates where the scan range is enlarged. Scan size: a-b)  $72 \times 72 \text{ nm}^2$ ; c-d)  $172 \times 172 \text{ nm}^2$ . Imaging conditions:  $V_{\text{bias}} = -600 \text{ mV}$ ,  $I_{\text{set}} = 330 \text{ pA}$ .

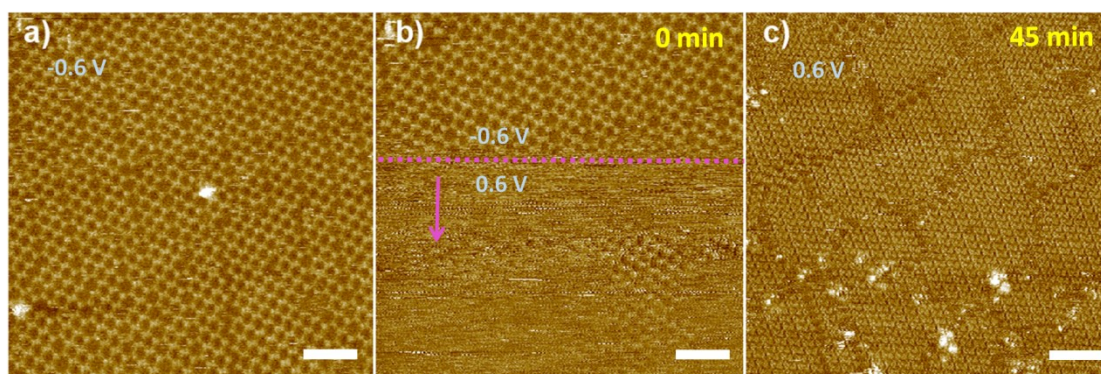


Figure S11. Sequential STM images showing the transition between cocrystal A and close packed BTB lamellae achieved by reversing the polarity of the substrate bias. Imaging conditions:  $V_{\text{bias}} = -600 \text{ mV}$ ,  $I_{\text{set}} = 330 \text{ pA}$ . Scale bars: 10 nm.

#### References:

- [1] A. D. Becke, *J. Chem.Phys.* **1993**, *98* (7), 5648-565.
- [2] B. Miehlich, A. Savin, H. Stoll, H. Preuss, *Chem. Phys. Letts.* **1989**, *157* (3), 200-206.
- [3] C. Lee, W. Yang, R. G. Parr, *Phys Rev. B* **1988**, *37* (2), 785-789.
- [4] M. J. Frisch, G. W. Trucks, H. B. Schlegel, G. E. Scuseria, M. A. Robb, J. R. Cheeseman, et al. Gaussian 03, Revision D.02. Gaussian Inc.; 2004.
- [5] R. Dennington II, T. Keith, J. Millam. GaussView, version 4.1.2. Semichem Inc.; 2007.